SUPPLEMENTARY DATA

Materials. Recombinant human insulin, calcein, actinomycin D, BrdU, and deoxyribonuclease were from Sigma. The Akt inhibitor MK2206 was from Selleck Chemicals. The PI3K inhibitor LY294002 and the cell-permable free radical scavenger 4-hydroxy-2,2,6,6-tetramethylpiperidine-1-oxyl (TEMPOL) were from Calbiochem. The cell-permable cGMP agonist 8-(4-chlorophenylthio)-cGMP (8-pCPT-cGMP) and the cGMP antagonist 8-(4-chlorophenylthio)-b-phenyl-1,N2-ethenoguanosine-3',5'-cyclic monophosphorothioate, Rp isomer (Rp-CPT-PET-cGMPS) were from Biolog. The NOS inhibitor N-nitro-L-arginine methyl ester (L-NAME), the sGC inhibitor 1*H*-[1,2,4] oxadiazolo[4,3-*a*] quinoxalin-1-one (ODQ), metformin, and the TBARS assay kit to measure malondialdehyde concentrations were obtained from Cayman. The sGC activator cinaciguat (BAY 58-2667) was from AdipoGen, and the sGC stimulator riociguat (BAY63-2521) was from Haoyuan Chemexpress. The Amplex Red Hydrogen Peroxide/Peroxidase Assay Kit and MitoSOX Red was from Thermo Fischer Scientific. The Nitric Oxide Quantitation Kit was from Active Motif, the cGMP ELISA was from Biomedical Technologies, and the CTX ELISA was from MyBiosource Inc. The Oxyblot™ Protein Oxidation Detection Kit was from EMD Millipore. Adenoviral vectors encoding β-galactosidase (LacZ), green fluorescent protein (GFP), and shRNA targeting human *nox4* were generated in the UCSD Viral Core. Adenovirus encoding OGT and GCA were previously described (Clark et al., 2003). Antibodies are summarized in Supplemental Table 2. Mycoplasma infection of cultured cells was excluded using MycoAlert™ (Lonza).

Supplementary Figure 1. Insulin effects on NO production and survival in murine POBs. (a) Murine osteoblasts were isolated from control mice and cultured in medium containing 25 mM glucose. Cells were transferred to fresh medium and pre-treated for 1 h with vehicle, 10 μM LY294002, or 10 μM MK2206 prior to stimulation with insulin for 20 min. Nitrite and nitrate (stable NO metabolites, NO_x) were measured as in Fig. 1a (mean ± SD of three independent experiments, ***$p<0.001$ for the indicated comparisons by ANOVA). **(b)** *prkg2*$^{f/f}$ POBs were infected with LacZ or CRE virus, and 30 h later were cultured in medium containing 10% FBS (full medium) or 0.1% BSA (serum starvation) for 18 h in the presence or absence of insulin; apoptosis was assessed by immunofluorescence staining for cleaved caspase-3 as described in Fig. 1i. Shown here is a separate experiment from that shown in Fig. 1i, and photographs were taken with 10x magnification.

©2018 American Diabetes Association. Published online at http://diabetes.diabetesjournals.org/lookup/suppl/doi:10.2337/db17-0965/-/DC1

SUPPLEMENTARY DATA

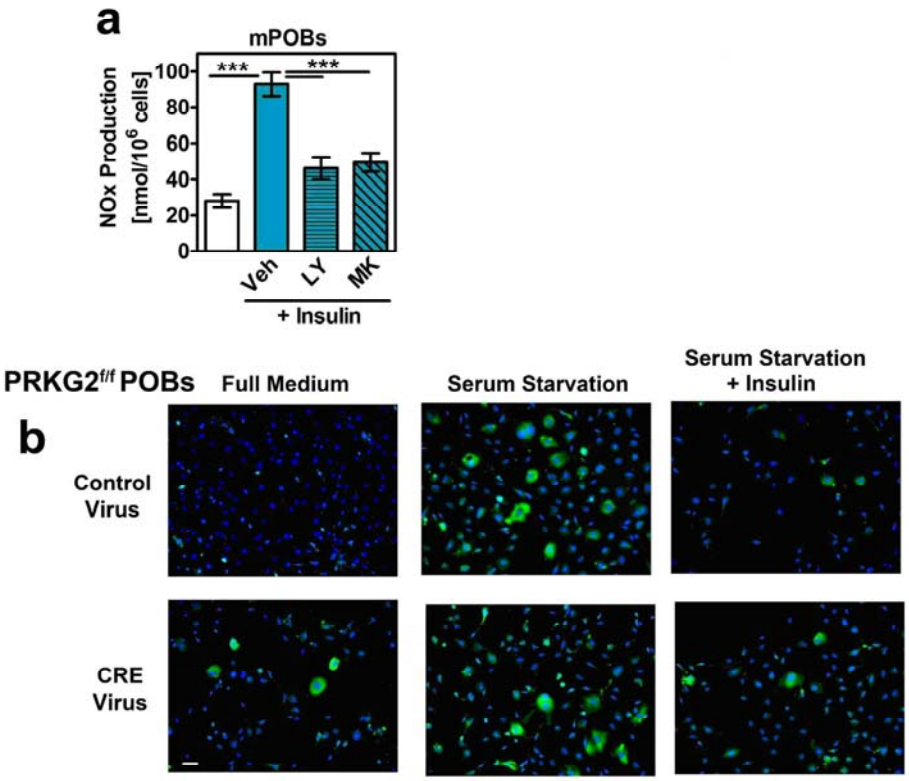

©2018 American Diabetes Association. Published online at http://diabetes.diabetesjournals.org/lookup/suppl/doi:10.2337/db17-0965/-/DC1

SUPPLEMENTARY DATA

Supplementary Figure 2. Lack of mannitol effect on insulin-induced ERK and Akt activation; effect of high glucose on GlcNAc modification of NOS3 and on NO production. (a-c) Human POBs isolated from non-diabetic individuals were cultured for three weeks in medium containing 5 mM glucose (LG), 25 mM glucose (HG), or 5 mM glucose plus 20 mM mannitol. Cells were stimulated with insulin for 10 min, and ERK1/2 and Akt phosphorylation were assessed by Western blotting using phospho-specific antibodies and quantified by densitome-try scanning as described in Fig. 1b. **(d)** Human POBs (left) or UMR106 rat osteoblastic cells (right) were cultured in LG or HG as in a, and NOS3 was isolated by 2',5'-ADP-agarose pull-down. O-GlcNAc modifi-cation was assessed by Western blotting with RL-2 antibody, and total NOS3 bound was assessed by re-probing with a NOS3-specific antibody. Three independent experiments with human POBs are summarized in Fig. 2f. **(e)** POBs were isolated from mice with streptozotocin-induced type 1 diabetes (T1DM) in medium containing 25 mM glucose (HG). After the first passage, cells were switched to media containing either 5 mM (LG) or 25 mM (HG) glucose, and were plated in the same media for each time point at a density of $2x10^4$ cells/cm^2. Accumulation of stable NO metabolites (nitrites and nitrates, NOx) was measured two hours after transfer to fresh medium as described in Fig. 2f. **(f,g)** POBs were isolated from control mice and cultured in LG or HG for 3 weeks prior to being infected for 48h with control virus (LacZ), virus encoding O-GlcNAc transferase (OGT) or N-acetylgluco-saminidase (GCA); OGT and GCA add or remove O-GlcNAc, respectively. NO_x was measured 2 h after adding fresh medium (e), and OGT and GCA expression was assessed by Western blotting (f). Data in graphs are means ± SD of at least three independent experiments; by ANOVA, *$p<0.05$, **$p<0.01$, and ***$p<0.001$ for the indicated comparisons, $^{\#\#}p<0.01$ and $^{\#\#\#}p<0.001$ for comparison between HG *versus* LG medium with insulin.

©2018 American Diabetes Association. Published online at http://diabetes.diabetesjournals.org/lookup/suppl/doi:10.2337/db17-0965/-/DC1

SUPPLEMENTARY DATA

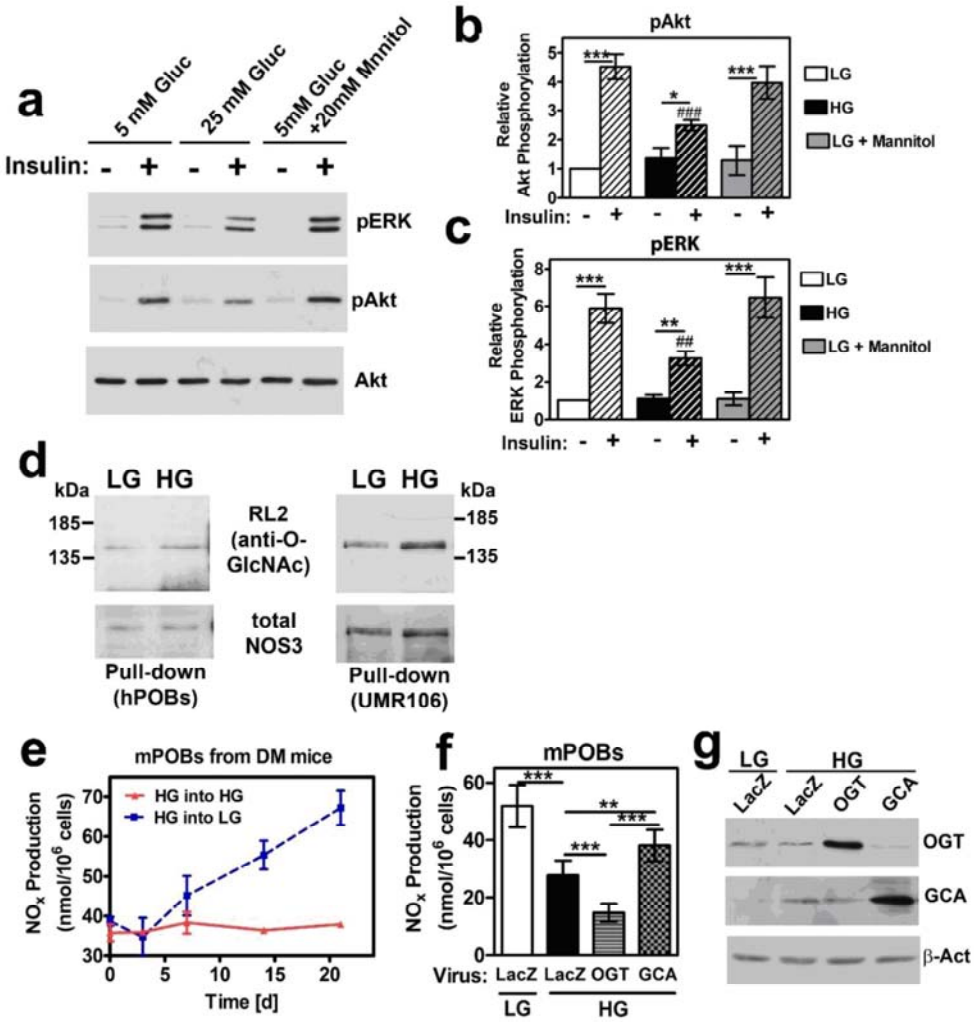

©2018 American Diabetes Association. Published online at http://diabetes.diabetesjournals.org/lookup/suppl/doi:10.2337/db17-0965/-/DC1

SUPPLEMENTARY DATA

Supplementary Figure 3. *prkg1*/2 mRNA stability is the same in low and high glucose medium; tempol increases *prkg1*/2 mRNA expression while decreasing lipid peroxidation in POBs cultured in high glucose. (a,b) Human POBs were cultured for 3 weeks in 5 mM or 25 mM glucose as in Fig. 3j, and *prkg1* (a) and *prkg2* (b) mRNA stability was measured by qRT-PCR after the addition of actinomycin D (1 µg/ml). Relative amounts of mRNA measured in low glucose or high glucose at the time of actinomycin addition (time 0) were assigned a value of 100% to allow direct comparison of mRNA decay. Data are the means ± SD of two independent experiments performed in duplicate. **(c,d)** Murine osteoblasts from control mice were cultured for 3 weeks in low glucose (LG) or high glucose (HG) , and some cells received tempol as described in Fig. 3k. *prkg1* and 2 mRNA abundance was measured by qRT-PCR (c), and lipid peroxidation was assessed by measuring malondialdehyde (MDA) concentrations as described in Methods (d). Data are means ± SD of three independent experiments; by ANOVA, *p<0.05 and ***p<0.001 for the indicated comparisons.

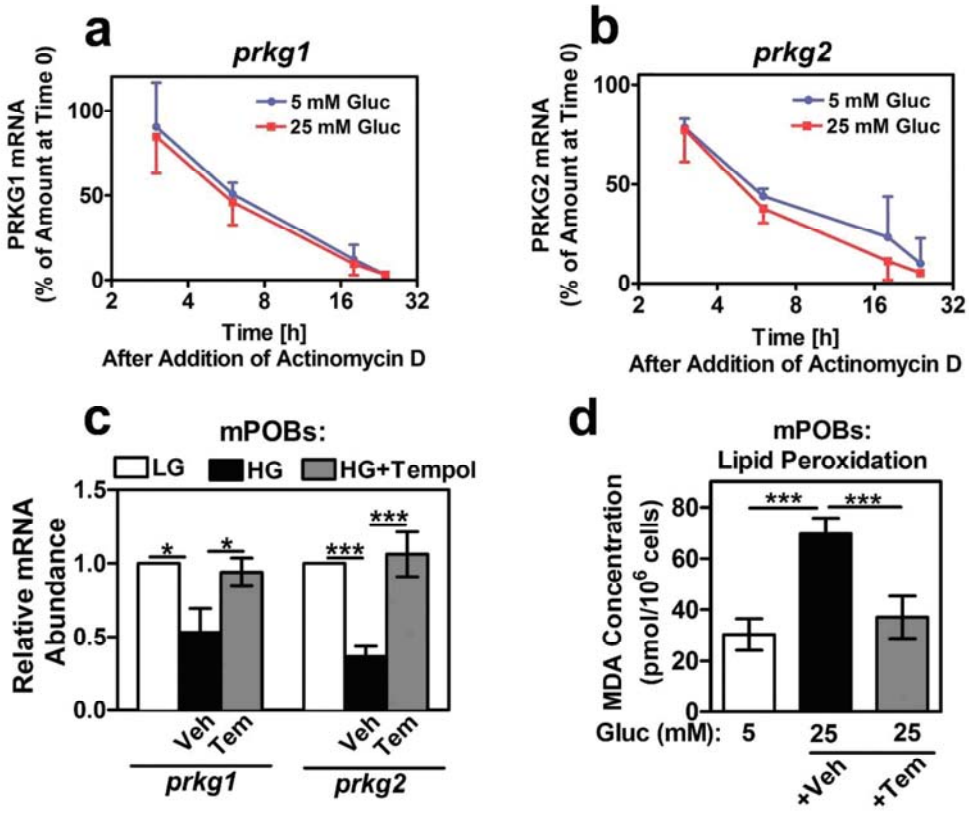

©2018 American Diabetes Association. Published online at http://diabetes.diabetesjournals.org/lookup/suppl/doi:10.2337/db17-0965/-/DC1

SUPPLEMENTARY DATA

Supplementary Figure 4. Cinaciguat treatment restores osteoblastic differentiation of bone marrow stromal cells isolated from diabetic mice. Bone marrow stromal cells were isolated from control mice, STZ-treated diabetic mice (DM), or diabetic mice treated with cinaciguat (DM+Cin) as described in Fig. 4. Cells were cultured in osteoblastic differentiation medium containing 5 mM (control) or 25 mM glucose (DM), and cells from cinaciguat-treated mice received 100 nM of the drug in the medium, as described in Fig. 5f. Colonies were stained for ALP activity after 14 d.

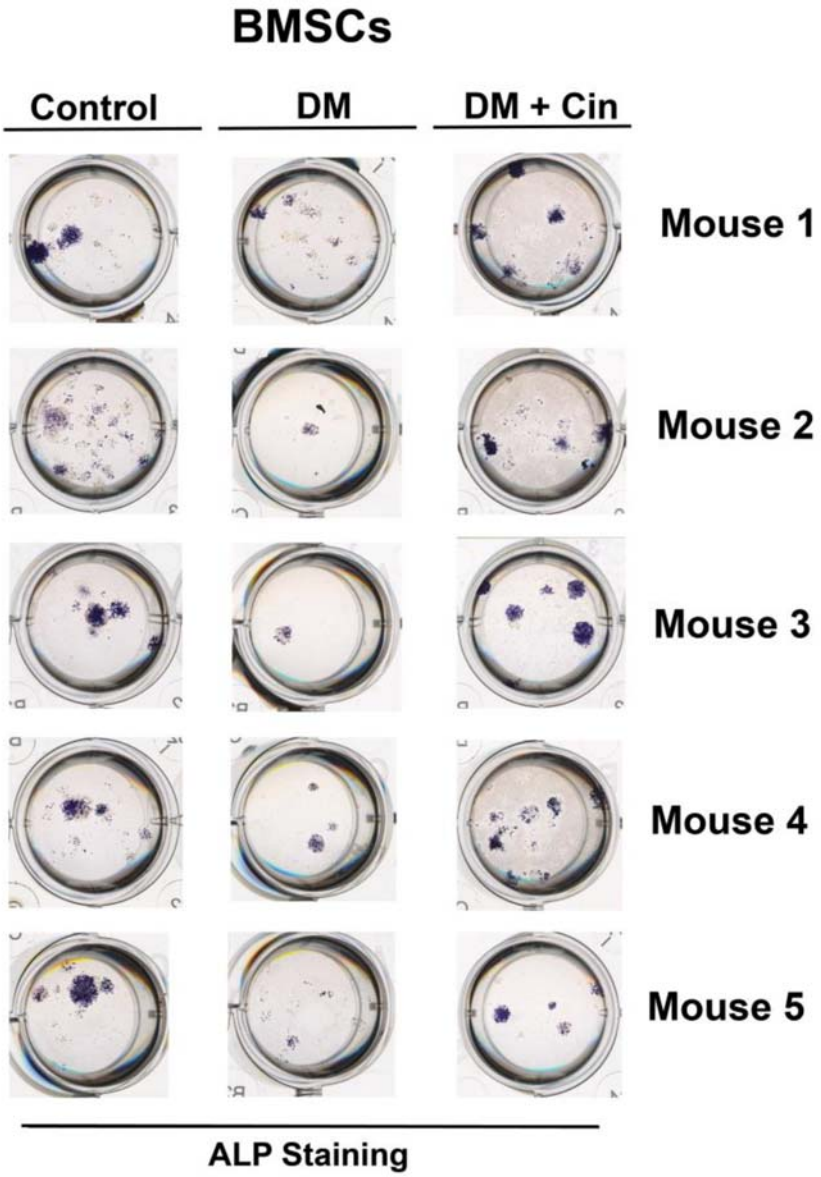

©2018 American Diabetes Association. Published online at http://diabetes.diabetesjournals.org/lookup/suppl/doi:10.2337/db17-0965/-/DC1

SUPPLEMENTARY DATA

Supplementary Figure 5. Cinaciguat reduces high glucose-induced JNK and p38 activation and mitochon-drial O_2^- production; uncoupled NOS activity does not contribute to H_2O_2 production by POBs in low or high glucose medium. (a-c) POBs isolated from control mice, diabetic mice, or diabetic mice treated with cinaciguat were cultured in 5 mM glucose (Con), 25 mM glucose (DM), or 25 mM glucose plus 0.1 μM cina-ciguat (DM+Cin), respectively, and p38 and JNK activation were assessed by Western blotting with phospho-specific antibodies and quantified by densitometry scanning of Western blots. **(d)** Human POBs were cultured in 5 mM glucose (LG) or 25 mM glucose (HG) for 3 weeks, and treated with the NOS inhibitor L-NAME (4 μM) overnight before measuring H_2O_2 production by Amplex Red fluorescence as in Fig. 5b. **(e)** Human POBs were cultured in LG or HG for 3 weeks; some cells in HG received cinaciguat (Cin, 0.1 μM) for the last 48 h, and some cells in LG were treated with Antimycin A (4 μM) for 18 h. Cells were loaded with the mitochondrial O2- indicator MitoSOX Red and nuclei were stained with Hoechst 33342 (blue). Antimycin A inhibits complex III, leading to increased mitochondrial O_2^- production, and served as a positive control. Bar graphs represent means ± SD of three independent experiments; by ANOVA, **p<0.01 and ***p<0.001 for the indicated comparisons.

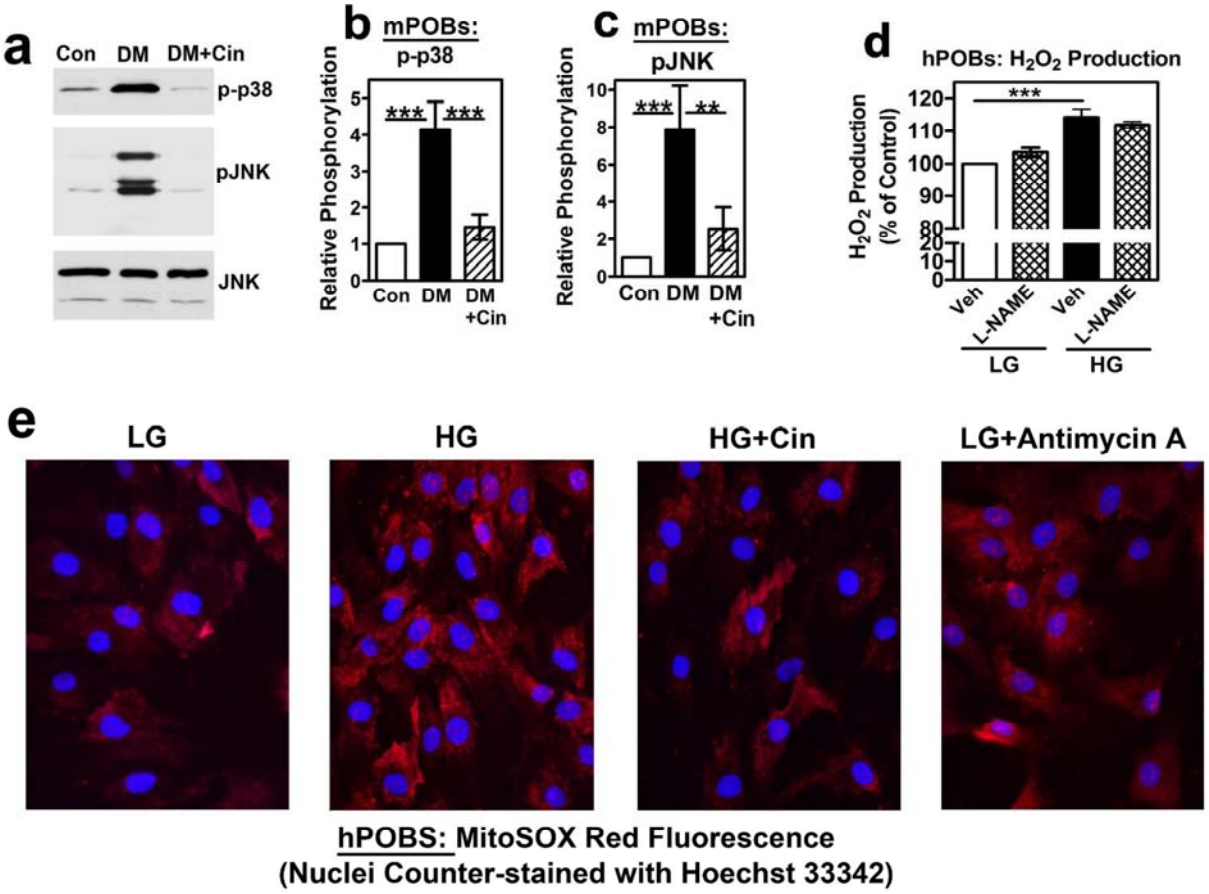

©2018 American Diabetes Association. Published online at http://diabetes.diabetesjournals.org/lookup/suppl/doi:10.2337/db17-0965/-/DC1

SUPPLEMENTARY DATA

Supplementary Figure 6. Cinaciguat reduces high glucose-induced NOX4 expression; cinaciguat does not affect *nox4* and *txn1* mRNA expression in low glucose-containing medium. (a,b) Human POBs were cultured in 5 mM glucose (LG) or 25 mM glucose (HG) for three weeks; some cells in HG received 0.1 μM cinaciguat (HG+Cin) for the last 48 h. NOX4 protein expression was assessed by Western blotting and quantified by densitometry. **(c,d)** Human POBs were cultured in 5 mM glucose (LG) for at least 3 weeks; some cells received 0.1 μM cinaciguat (Cin), 100 μM 8-CPT-cGMP (cGMP), or 200 μM tempol (Tem) for the last 48 h, as indicated. *nox4* and *txn1* mRNAs were quantified by RT-PCR and normalized to 18S rRNA as in Fig. 6d and f; expression in control, vehicle-treated POBs was assigned a value of one**.** Graphs represent means ± SD of at least three independent experiments; by ANOVA, **p<0.01 and ***p<0.001 for the indicated comparisons in b.

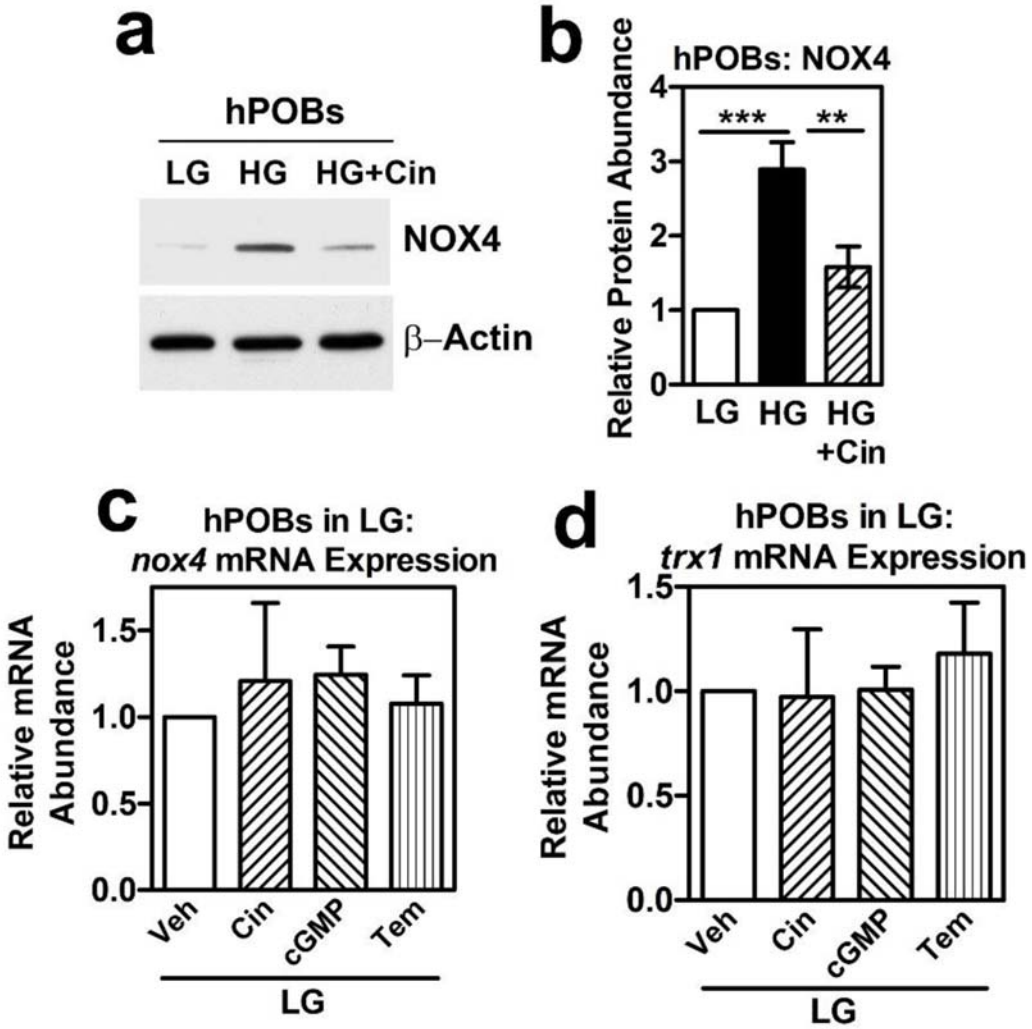

©2018 American Diabetes Association. Published online at http://diabetes.diabetesjournals.org/lookup/suppl/doi:10.2337/db17-0965/-/DC1

SUPPLEMENTARY DATA

Supplementary Figure 7. Cinaciguat effects on cortical osteoblast number, osteocycte apoptosis, and bone marrow adiposity in diabetic mice. T1DM was induced in 12 week old male C57Bl/6 mice as described in Fig. 7a. **(a)** Osteoblasts were counted on endocortical surfaces **(b)** Osteocyte apoptosis was assessed by TUNEL staining of femoral cortex sections. Cells with black nuclear stain were counted, and results of 6-7 mice per group were summarized in Fig. 7l. **(c,d)** Sections of methylmethacrylate-embedded femurs were stained with Masson's trichrome (the bar represents 500 µm, at 4 x magnification). A representative area 0.25 mm distal to the growth plate is shown enlarged (at 12 x magnification). Fat cells appear as clear round spaces. The % area occupied by adipose cells was measured in an area between 0.25 and 2.25 mm distal to the growth plate (d). N=6-7 mice per group; *p<0.05 and ***p<0.001 for the indicated comparisons (by ANOVA).

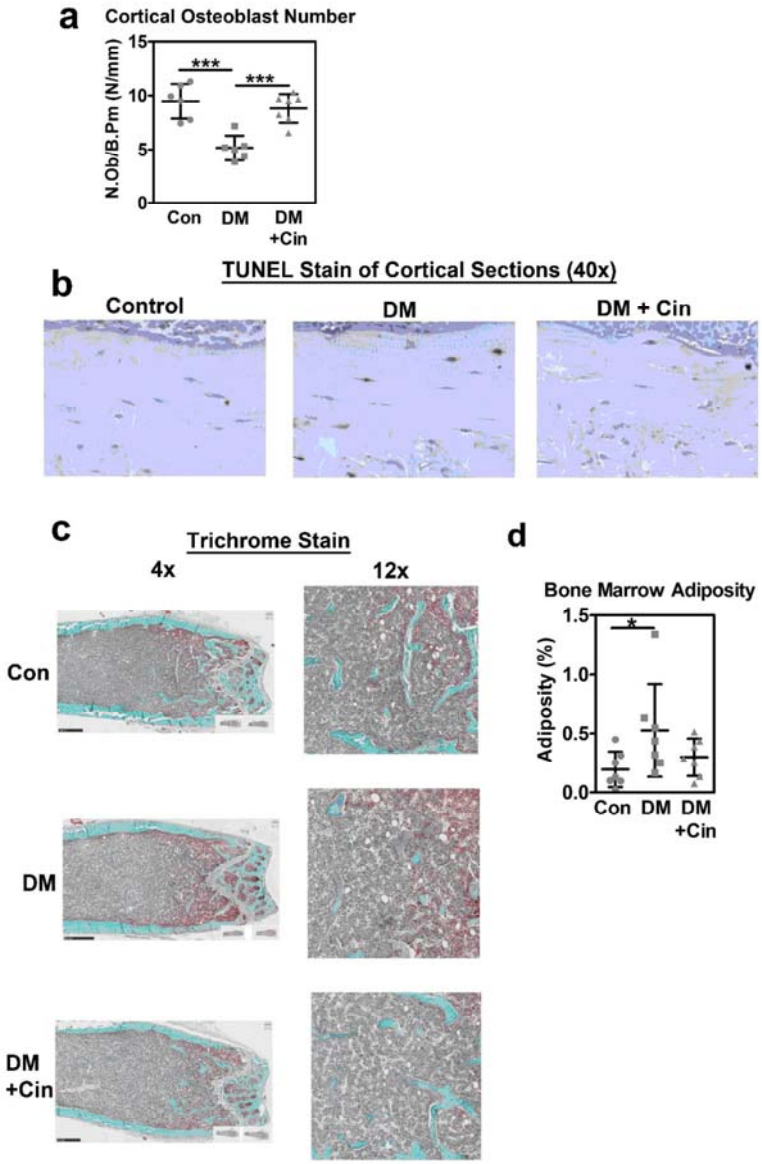

©2018 American Diabetes Association. Published online at http://diabetes.diabetesjournals.org/lookup/suppl/doi:10.2337/db17-0965/-/DC1

SUPPLEMENTARY DATA

Supplementary Figure 8. Cinaciguat effect on VEGF-A expression and microvessel density in diabetic mice. (a) Vascular endothelial growth factor A (*vegfa*) mRNA expression was measured in tibial bone as described in Fig. 7c. **(b,c)** Sections of methylmethacrylate-embedded femurs were stained with anti-CD31 antibody followed by anti-mouse HRP-coupled antibody and incubation with DAB substrate; cells were counter-stained with hematoxylin (b). Clusters of at least two endothelial cells with membrane anti-CD31 staining were defined as a microvessel and counted in an area between 0.25 and 2.25 mm distal to the growth plate to determine capillary density (c). N=5-7 mice per group; *p<0.05, **p<0.01, ***p<0.001 for the indicated comparisons (by ANOVA).

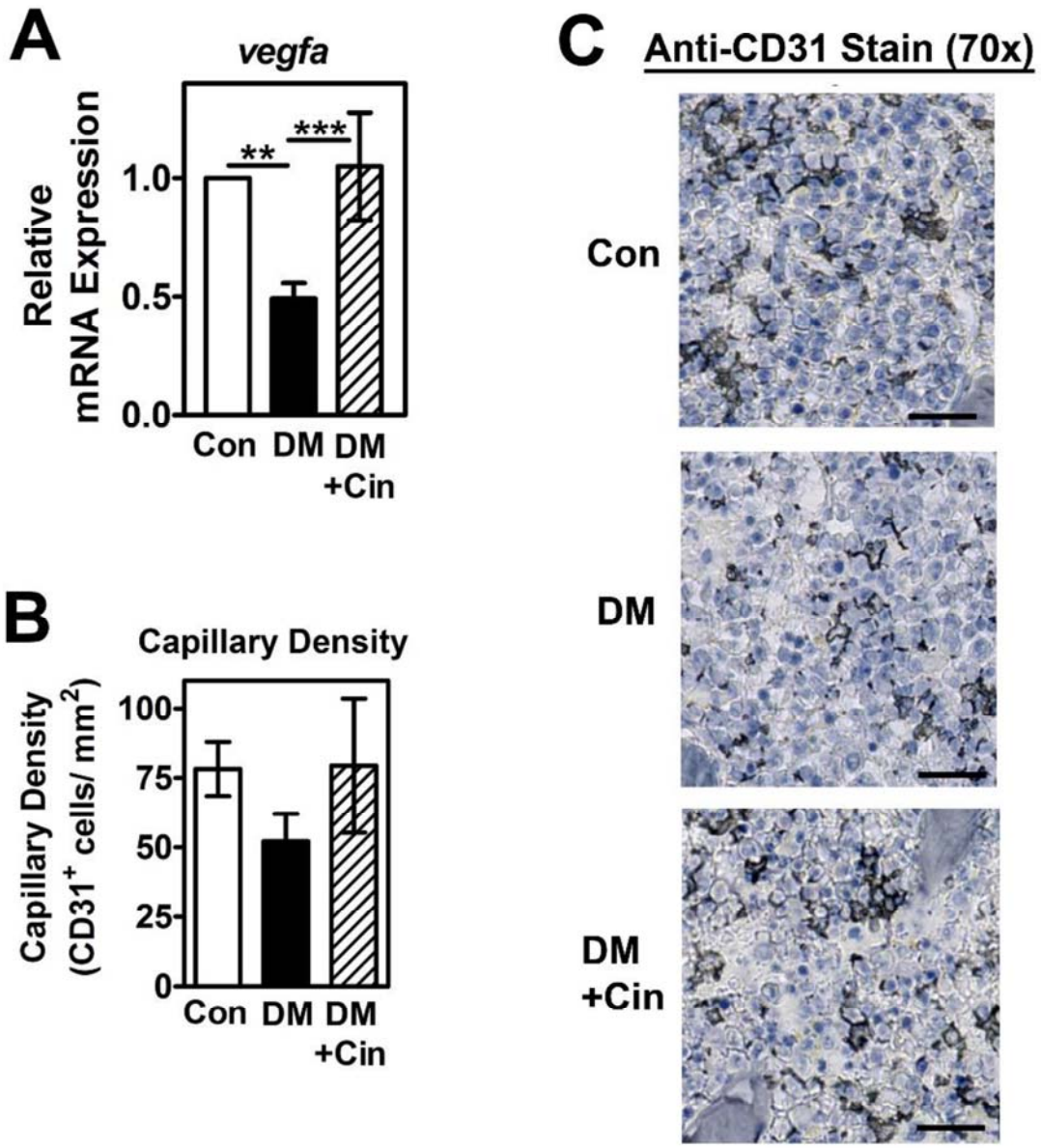

©2018 American Diabetes Association. Published online at http://diabetes.diabetesjournals.org/lookup/suppl/doi:10.2337/db17-0965/-/DC1

SUPPLEMENTARY DATA

Supplementary Table 1. Blood Glucose and Body Weight Measurements

Mice were injected with streptozotocin (DM) or vehicle (Control) for 5 d, and 13 d after the start of injections, blood glucose was measured as described in Fig. 8a. Diabetic mice (blood glucose >270 mg/dl) received vehicle or cinaciguat from d 21 through d 48, and mice were euthanized 1 h after the last injection. Controls, n=9; DM, n=8; DM+Cin, n=10; ***p,0.001 for the comparison to the control group.

Group	Blood Glucose (mg/dl) Day 13	Blood Glucose (mg/dl) Day 48	Body Weight (g) Day 48
Control	143.4 ± 5.1	134.8 ± 2.5	24.7 ± 0.4
DM	345.6 ± 29.8***	445.0 ± 17.9***	23.9 ± 0.4
DM + Cinaciguat	348.4 ± 19.2***	480.1 ± 11.1***	23.3 ± 0.3

©2018 American Diabetes Association. Published online at http://diabetes.diabetesjournals.org/lookup/suppl/doi:10.2337/db17-0965/-/DC1

SUPPLEMENTARY DATA

Supplementary Table 2. Antibodies Used for Western blotting (WB), Immunofluorescence (IF), Immunohistochemistry (IHC), and Immunoprecipitation (IP).

©2018 American Diabetes Association. Published online at http://diabetes.diabetesjournals.org/lookup/suppl/doi:10.2337/db17-0965/-/DC1

SUPPLEMENTARY DATA

Antibody Target	Catalog number	Source	Dilution	
β-actin	SC47778	Santa Cruz Biotechnology	WB 1:5000	
Akt (pSer473)	9271S	Cell Signaling	WB 1:1000	
Akt	9272S	Cell Signaling	WB 1:1000	
BrdU	B8434	Sigma-Aldrich	IF 1:200	
Caveolin-1 (rabbit)	3267P	Cell Signaling	WB 1:2000	
CD31 (PECAM-1)	SC376764	Santa Cruz Biotechnology	IHC 1:100	
Cleaved caspase-3	9664S	Cell Signaling	IF 1:100	
ERK1 (pY204)	4376S	Cell Signaling	WB 1:5000	
sGC	160897	Cayman Chemical	WB 1:1000	
Hsp90	4874S	Cell Signaling	WB 1:1000	
8-OH-deoxyguanosine	ab62623	Abcam	IF 1:100	
JNK (pT183/Y185)	4668S	Cell Signaling	WB 1:2000	
JNK	9252S	Cell Signaling	WB 1:5000	
NOS 3	SC-654	Santa Cruz Biotechnology	WB 1:500	IP 1:500
NOS 3 (pS1177)	9571S	Cell Signaling	WB 1:1000	
NOX 4	ab60940	Abcam	WB 1:1000	
NOX 2	ab129068	Abcam	WB 1:1000	
OGT	ab177941	Abcam	WB 1:1000	
PKGI	3248S	Cell Signaling	WB 1:1000	
PKGII	AP8001a	Abgent	WB 1:1000	
p38 (pT180/Y182)	9211S	Cell Signaling	WB 1:2000	
RL-2 (anti-O-GlcNAc)	Ab2739	Abcam	WB 1:1000	
α-Tubulin	SC-8035	Santa Cruz Biotechnology	WB 1:1000	

©2018 American Diabetes Association. Published online at http://diabetes.diabetesjournals.org/lookup/suppl/doi:10.2337/db17-0965/-/DC1

SUPPLEMENTARY DATA

Supplementary Table 3. Murine Primer Sequences Used for Quantitative RT-PCR

All primer pairs were tested with serially-diluted cDNAs and were intron-spanning (except 18S primers, which were tested with and without reverse transcriptase to rule out genomic DNA contamination).

Abbrev	Gene Name	Sense Primer (5'-3')	Anti-sense Primer (5'-3')
alpl	Alkaline Phosphatase	TCAGGGCAATGAGGTCACATC	CACAATGCCCACGGACTTC
bglap	Osteocalcin	GAGGACCATCTTTCTGCTCAC	CCAAGGTAGCGCCGGAGTCTG
c-fos	c-Fos	CGCAGAGCATCGGCAGAAGG	TCTTGCAGGCAGGTCGGTGG
gucy1	Soluble Guanylate Cyclase β	AAGGAGCACTTCTTTCCCTGTG	ACAAACTTAACACAGTGGGTGC
ssp1	Osteopontin	CCAGGTTTCTGATGAACAGTATCC	ACTTGACTCATGGCTGCCCTTT
lrp5	Low-density Lipo-protein Receptor-related Protein 5	ACTCACGGGTGTCAAAGAGG	AGGGTAGTCGAGGCCAAACT
nos3	Nitric oxide Synthase 3	TACGCACCCAGAGCTTTTCT	CTTGGTCAACCGAACGAAGT
nox 2	NADPH Oxidase 2	AAGACTCTGTATGGACGGCC	GCCGGATTCTGAGTTGGAGA
nox 4	NADPH Oxidase 4	GGCAAGAAAACAGACCTGACT	GACGCCCAATGAAAAGTCTC
prkg1	Protein Kinase G 1	GTCACTAGGGATTCTGATGTATGA	TTTGCAATCTTCTTTGGAAATTCT
prkg2	Protein Kinase G 2	GAGAGTACTTTGGAGAAAAGG Or set 2: GTGACACAGCGCTGGTTGTT	GTTTGGTTGAATGTTTCTCT Or set 2: TGGGAATGGAAAAGGACAAC
runx2	Runx-related Transcription Factor 2	GACAGAAGCTTGATGACTCTAAACC	TCTGTAATCTGACTCTGTCCTTGT
18S	18S ribosomal RNA	GAACGTCTGCCCTATCAACT	CCAAGATCCAACTACGAGCT
tuba1	Tubulin, alpha 1A	CCGCGAAGCAGCAACCAT	CCAGGTCTACGAACACTGCC
txn1	Thioredoxin1	TATAAAGAGAAGGCGGGCG	AGAAGTCCACCACGACAAG
txnrd1	Thioredoxin reductase 1	TGAGCTGCCGAACAAAAAAG	ATCTGGTCCCAAGAGGAGTC
prdx1	Thioredoxin peroxidase 1	CATTGCTCAGGATTATGGAGTC	CATTTATTGTTATCTGGCGAAGG
txnip1	Thioredoxin interacting protein 1	CGCTATGAAGACACACTTCTC	CGAAGCCGAACTTGTACTC

©2018 American Diabetes Association. Published online at http://diabetes.diabetesjournals.org/lookup/suppl/doi:10.2337/db17-0965/-/DC1

SUPPLEMENTARY DATA

Supplementary Table 4. Human Primer Sequences Used for Quantitative RT-PCR

Abbrev	Gene Name	Sense Primer (5'-3')	Anti-sense Primer (5'-3')
nox 4	NADPH Oxidase 4	TCATGCACTGAATTGAAGAC	TGTCCCATATGAGTTGTTCT
prkg1	Protein Kinase G 1β	CACCTTGCGGGATTTACAGT	GTAGAAGGGCAGGGTCACAT
prkg2	Protein Kinase G 2	AAGCACCCAGATGGACACTC	TCAGCTGGATGCACTTGTTC
tuba1	Tubulin, alpha 1	TTGGCCAGATCTTTAGACCAGAC AAC	CCGTACCACATCCAGGACAGA ATC
txn1	Thioredoxin1	GATGTGGATGACTGTCAGGATGT	TCACCCACCTTTTGTCCCTTC

©2018 American Diabetes Association. Published online at http://diabetes.diabetesjournals.org/lookup/suppl/doi:10.2337/db17-0965/-/DC1